phys. stat. sol. (b) **141**, 129 (1987)

Subject classification: 71.38 and 71.45; 68.30; 73.40; 77.30; 78.65; S7.12; S7.15

Sektion Physik der Friedrich-Schiller-Universität Jena[1])

Dynamical Screening, Collective Excitations, and Electron–Phonon Interaction in Heterostructures and Semiconductor Quantum Wells

Application to Double Heterostructures[2])

By

L. WENDLER and R. PECHSTEDT

The collective excitations of a double heterostructure are examined in detail. Including the important effects of the interfaces of the system the uncoupled modes are analysed, which are the long-wave optical interface phonon modes, LO phonon modes, and intra- and intersubband plasmon modes. The electron–phonon interaction is discussed and the coupling functions are calculated and discussed in graphical form. The resulting coupled modes, intra- and intersubband plasmon–phonon modes, are calculated for different approximations of the polarization function, the random-phase approximation, the plasmon-pol approximation, and the long-wave approximation. The dispersion curves of these modes are presented in graphical form for various cases. It is shown that the Landau damping of the modes strongly depends on the layer thickness and the concentration of the quasi-two-dimensional electron gas.

Die kollektiven Anregungen einer Doppelheterostruktur werden ausführlich untersucht. Es werden die ungekoppelten Moden, d. h. die langwellig-optischen Grenzflächen-Phononen, die LO-Phononen sowie die Intra- und Intersubband-Plasmonen unter Einbeziehung der Grenzflächeneffekte diskutiert. Im Detail werden die Elektron–Phonon-Wechselwirkung analysiert, die Kopplungsfunktionen berechnet und graphisch dargestellt. Die resultierenden gekoppelten Moden, die Intra- und Intersubband-Plasmon–Phononen werden für mehrere Näherungen der Polarisationsfunktion, der Random-Phase-Approximation, der Plasmon-Pol-Näherung und der langwelligen Näherung berechnet. Die Dispersionskurven sind für verschiedene Fälle graphisch dargestellt. Es wird gezeigt, daß die Landau-Dämpfung der Moden stark von der Schichtdicke und der Konzentration des quasi-zweidimensionalen Elektronengases abhängt.

1. Introduction

In the last few years the interest in the investigation of interface properties of condensed media and of thin layer properties, especially of semiconductors, has been highly increased. Solid state surfaces as well as interfaces between two media are connected with a variety of interesting phenomena. On the one hand, their existence results in completely novel effects and, on the other hand, the properties of the bulk are changed. The advantages of the crystal growth techniques metal–organic chemical-vapour deposition and molecular-beam epitaxy made it possible to produce a high mobility quasi-two-dimensional electron gas (Q2DEG) in a variety of semiconductor devices. The scope of studying Q2D confined charge carriers has been highly enhanced by the advance made by the modulation doping technique. Selective doping of the

[1]) Max-Wien-Platz 1, DDR-6900 Jena, GDR.

[2]) General theory see, phys. stat. sol. (b) **138**, 197 (1986).

wider gap semiconductor produces a high mobility Q2DEG in the smaller gap semiconductor. The Q2DEG is spatially separated from the parent ionized impurities and hence the ionized impurity scattering is drastically reduced.

Double heterostructures (DHS or single quantum well) are important for a large field of semiconductor devices. These microstructures are typified by a square-well potential formed by a layer of the smaller gap semiconductor buried in the bulk of the wider gap semiconductor (Fig. 1 and 2). Hence, the quasi-free electrons are confined to the smaller gap semiconductor layer forming a Q2DEG. Since these DHS's are mostly composed of the weakly polar compound semiconductor materials of the III–V series, both electron–electron and electron–phonon interactions take place. Electron–phonon interaction in such materials is mainly polar in nature, that means the long-wave optical lattice vibrations which are accompanied by macroscopic electric fields, couple to the electrons of the Q2DEG.

The interfaces of the system alter the spectrum of the long-wave optical phonons of the bulk case. First, the bulk properties of the longitudinal optical (LO) phonons are changed by the interference of incident and backscattered waves. This yields a vanishing influence of these long-wave optical lattice vibrations at the boundaries of the DHS. Second, new states in the spectrum of the long-wave optical phonons occur: interface phonons. The electrons of the Q2DEG interact with both, LO and interface phonons. Therefore, the collective excitations of the DHS are coupled states of the charge-density fluctuations of the Q2DEG and the different long-wave optical phonons.

In the last time a lot of papers appeared concerning with dielectric screening, collective excitations, and electron–phonon interaction in semiconductor quantum wells and superlattices [1 to 6, 11 to 13]. In these papers the optical phonon system is taken into account in different ways. Some authors [1 to 6] treat the contribution of the optical phonons only by a background dielectric constant (ε_s-approximation) or the coupling is treated only to the ordinary 3D bulk LO phonons. In these works the important effect of the interfaces is neglected. Surface effects have been intensively studied for the case of plasmons in semi-infinite metals [7 to 10], but only a small part of works on collective excitations in semiconductor quantum wells and superlattices include the effect of the interfaces [11 to 13]. In [11] we gave a general treatment of electron–phonon interaction and collective excitations in microstructures using the continuum model for the long-wave optical phonons (both LO and interface phonons). That means the complete long-wave optical phonon spectrum of the layered structure must be taken into account to investigate the electron–phonon interaction. The authors of [13] used another approach than in [11 and 12] to introduce the existence of the interfaces. Using the model of specular electron reflection they derived the dispersion relation of the collective excitations in terms of the bulk dielectric functions of the media including spatial dispersion.

Starting from the general treatment in [11] first results specified for a DHS are published in [12]. The aim of this paper is to give a more detailed representation of the electron–phonon interaction and collective excitations in DHS's. Furthermore, the influence of different approximations of the polarization function of the Q2DEG on the resulting dispersion relation of the collective excitations is investigated. The approximations studied are the long-wave approximation, the plasmon-pol approximation, and the random-phase approximation.

2. Electronic Subband Structure

The DHS (Fig. 1) which is under consideration in this paper consists of a smaller gap semiconductor (1) for $a > z > 0$ (for instance GaAs) which is symmetrically embedded

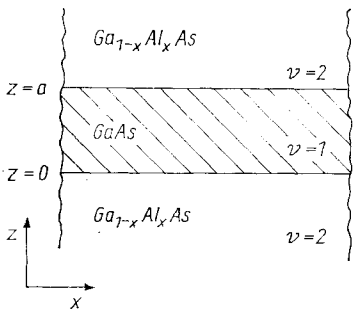

Fig. 1. Schematic arrangement of the geometry of a double heterostructure

between a wider gap semiconductor (2) for $z > a$ and $0 > z$ (for instance $Ga_{1-x}Al_xAs$). Due to the conduction band discontinuity at the two heterointerfaces at $z = 0$ and a the electrons can move quasi-free in the x–y plane, but their motion is confined in the z-direction. In the effective-mass approximation the one-electron motion is given by the equivalent Schrödinger equation [14]

$$\left(-\frac{\hbar^2}{2m}\Delta + V_{\text{eff}}(z)\right)\psi_{\boldsymbol{k}_{||}K}(\boldsymbol{x}) = \mathscr{E}_K(\boldsymbol{k}_{||})\,\psi_{\boldsymbol{k}_{||}K}(\boldsymbol{x}) \tag{1}$$

with $V_{\text{eff}}(z)$ the effective confining potential of the DHS consisting of the potential resulting from the conduction-band offset at the heterointerfaces, the Hartree potential, and the exchange-correlation potential. According to the symmetry of the DHS the one-electron wave function has the form

$$\psi_{\boldsymbol{k}_{||}K}(\boldsymbol{x}) = \frac{1}{\sqrt{A}}\,\mathrm{e}^{i\boldsymbol{k}_{||}\boldsymbol{x}_{||}}\,\varphi_K(z)\,, \tag{2}$$

where $\boldsymbol{x}_{||}$ and $\boldsymbol{k}_{||}$ are two-dimensional position and wave vector in the x–y plane, respectively. K refers to the subband index and A is the unit area in the x–y plane. The confinement of the electron motion in z-direction (in order of the de Broglie wavelength of the electron) leads to a sequence of Q2D subbands according to

$$\mathscr{E}_K(\boldsymbol{k}_{||}) = \mathscr{E}_K + \frac{\hbar^2 k_{||}^2}{2m}; \qquad K = 0, 1, 2, \ldots\,. \tag{3}$$

The envelope wave function $\varphi_K(z)$ for an electron in the K-th subband is given by the one-dimensional effective Schrödinger equation

$$\left(-\frac{\hbar^2}{2m}\frac{\mathrm{d}^2}{\mathrm{d}z^2} + V_{\text{eff}}(z)\right)\varphi_K(z) = \mathscr{E}_K\varphi_K(z) \tag{4}$$

with

$$\int \mathrm{d}z\,|\varphi_K(z)|^2 = 1\,. \tag{5}$$

For the analytic and numerical calculations in the following sections we are interested in the simplest model potential neglecting band-bending and exchange-correlation effects and in which the quantum well has infinite barriers,

$$V_{\text{eff}}(z) = \begin{cases} 0; & a > z > 0\,, \\ \infty; & \text{otherwise.} \end{cases} \tag{6}$$

Within this simple infinite square well potential model the envelope wave function is given by

$$\varphi_K(z) = \sqrt{\frac{2}{a}}\,\sin\left(\frac{\pi(K+1)}{a}\,z\right) \tag{7}$$

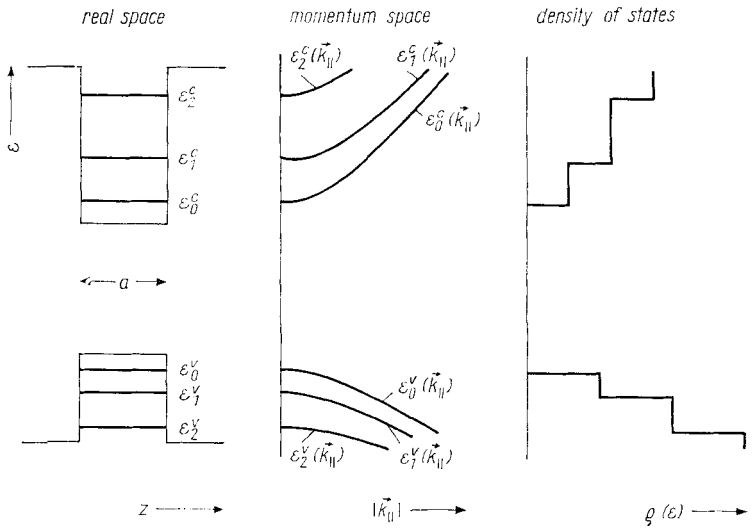

Fig. 2. Electronic subband structure of a double heterostructure formed by a thin layer of GaAs embedded between two semi-infinite $Ga_{1-x}Al_xAs$ semiconductors. In addition to the conduction band (c) also the valence band (v) is plotted (schematically, not to scale). The band bending at the heterointerfaces arising from the space charges is neglected

and the subband energies by

$$\mathscr{E}_K = \frac{\hbar^2\pi^2}{2ma^2}(K+1)^2 . \tag{8}$$

The *local density of states* is

$$\varrho(z, \mathscr{E}) = \frac{m}{\pi\hbar^2}\sum_K |\varphi_K(z)|^2\,\theta(\mathscr{E} - \mathscr{E}_K) , \tag{9}$$

where the unit step function $\theta(x) = 1$ for $x > 0$ and 0 for $x < 0$. The *density of states* for the DHS is then

$$\varrho(\mathscr{E}) = \frac{mA}{\pi\hbar^2}\sum_K \theta(\mathscr{E} - \mathscr{E}_K) . \tag{10}$$

The electronic subband structure and the density of states of a DHS are plotted in Fig. 2. According to the local density of states the electron number density $n(z)$ is given by

$$n(z) = \frac{mk_BT}{\pi\hbar^2}\sum_K |\varphi_K(z)|^2 \ln\left[1 + \exp\left(\frac{\mu - \mathscr{E}_K}{k_BT}\right)\right]. \tag{11}$$

The sheet carrier concentration n_{2DEG} (electron concentration per unit area) is obtained from (11) to

$$n_{2DEG} = \frac{mk_BT}{\pi\hbar^2}\sum_K \ln\left[1 + \exp\left(\frac{\mu - \mathscr{E}_K}{k_BT}\right)\right]. \tag{12}$$

This equation determines the chemical potential μ. In Tables 1 and 2 some results are given for the subband energies and the chemical potential of a GaAs–$Ga_{1-x}Al_xAs$ DHS.

Table 1
Subband energies of a GaAs–$Ga_{1-x}Al_xAs$ DHS

a (nm)	$\mathcal{E}_0$ (meV)	$\mathcal{E}_1$ (meV)	$\mathcal{E}_2$ (meV)
10	56.8	227.1	510.9
20	14.2	56.8	127.7
25	9.1	36.3	81.7
40	3.5	14.2	31.9

Table 2
Chemical potential of a GaAs–$Ga_{1-x}Al_xAs$ DHS

$n_{2\,\mathrm{DEG}}$ (10^{12} cm^{-2})	a (nm)	μ (meV)	
		$T = 0$ K	$T = 77$ K
0.1	10	60.4	54.6
0.1	20	17.8	12.0
0.1	25	12.7	6.8
0.1	40	7.2	−0.5
0.5	10	74.8	74.4
0.5	20	32.3	31.6
0.5	25	27.2	25.4
0.5	40	17.9	15.0
1.0	10	92.9	92.8
1.0	20	50.3	48.6
1.0	25	40.8	39.0
1.0	40	26.9	25.2

3. Long-Wave Optical Phonons and Electron–Phonon Interaction

The nature of the polar electron–phonon interaction is that the longitudinal part of the electric field which is connected with the long-wave optical phonons (polarization eigenmodes), interacts with the charge of the electron. The following investigation of this type of electron–phonon interaction in layered media follows quite closely the theory developed in [15]. Here we are only interested in this type of electron–phonon interaction under the assumption that the other interaction processes, such as piezoelectric interaction of electrons with acoustic phonons or the interaction via the deformation potential of electrons with acoustic or optical phonons, are unimportant for the interesting physics.

The coupling function of a single electron to the long-wave optical phonons of a multilayer system is given by [15]

$$\Gamma_j(\boldsymbol{q}_{||}, z) = -\frac{i}{q_{||}} \left(\frac{\varepsilon_0 e^2 \hbar}{2A\omega_j(\boldsymbol{q}_{||})} \right)^{1/2} E^j_{||}(\boldsymbol{q}_{||}, z) \,. \tag{13}$$

This function describes the coupling strength of a single electron at the position z with the j-th long-wave optical phonon mode in the layered structure which has the dispersion relation $\omega_j(\boldsymbol{q}_{||})$. $E^j_{||}(\boldsymbol{q}_{||}, z)$ denotes the longitudinal part of the electric field connected with the j-th long-wave optical phonon mode. As shown in [15] the long-wave optical phonons which interact with the electrons are the p-polarized LO

phonons and the interface phonons. The transverse optical (TO) phonons do not interact with the electrons. For the nonzero components of the p-polarized monochromatic electric field we use the two-dimensional Fourier series,

$$\boldsymbol{E}^j(\boldsymbol{x}, t) = \frac{1}{A} \sum_{\boldsymbol{q}_{||}} \mathrm{e}^{i(\boldsymbol{q}_{||}\boldsymbol{x}_{||} - \omega t)}\, \boldsymbol{E}^j(\boldsymbol{q}_{||}, z)\,. \tag{14}$$

Since the long-wave optical phonons are macroscopic normal modes, the lattice dynamical properties of the media of the DHS are completely described by its macroscopic lattice dielectric function which we assume to be

$$\varepsilon_\nu(\omega) = \varepsilon_{\infty\nu} \frac{\omega_{\mathrm{L}\nu}^2 - \omega^2}{\omega_{\mathrm{T}\nu}^2 - \omega^2}\,, \tag{15}$$

where $\nu = 1, 2$ denotes the material (see Fig. 1), $\varepsilon_{\infty\nu}$ is the optical dielectric constant, $\omega_{\mathrm{L}\nu}$ and $\omega_{\mathrm{T}\nu}$ are the longitudinal and transverse optical (LO and TO) phonon frequency, respectively. The amplitudes of the modes are orthonormalized according to

$$\int_{-\infty}^{\infty} \mathrm{d}z\, \frac{\theta_\nu^{1/2}(\omega_j)\, \theta_\nu^{1/2}(\omega_{j'})}{\omega_{\mathrm{p}\nu}^2}\, \boldsymbol{P}^{j*}(\boldsymbol{q}_{||}, z)\, \boldsymbol{P}^{j'}(\boldsymbol{q}_{||}, z) = \delta_{jj'} \tag{16}$$

with

$$\theta_\nu^{1/2}(\omega_j) = \frac{3\varepsilon_{\infty\nu}}{\varepsilon_{\infty\nu} + 2}\, \frac{\omega_{\mathrm{L}\nu}^2 - \omega_{\mathrm{T}\nu}^2}{\varepsilon_{\infty\nu}\left(\omega_{\mathrm{L}\nu}^2 - \omega_j^2(\boldsymbol{q}_{||})\right) - \left(\omega_{\mathrm{T}\nu}^2 - \omega_j^2(\boldsymbol{q}_{||})\right)} \tag{17}$$

and the ion plasma frequency

$$\omega_{\mathrm{p}\nu}^2 = \frac{9\varepsilon_{\infty\nu}}{(\varepsilon_{\infty\nu} + 2)^2}\, (\omega_{\mathrm{L}\nu}^2 - \omega_{\mathrm{T}\nu}^2)\,, \tag{18}$$

where the polarization field is given by $\boldsymbol{P}^j(\boldsymbol{q}_{||}, z) = \varepsilon_0 \chi_\nu(\omega_j)\, \boldsymbol{E}^j(\boldsymbol{q}_{||}, z)$. $\chi_\nu(\omega) = \varepsilon_\nu(\omega) - 1$ is the lattice dielectric susceptibility. In the following we discuss the interface and LO phonons of a DHS in detail.

3.1 Interface phonons

The interface phonons discussed here are long-wave optical phonons which owe their existence to the presence of the interfaces of the DHS. Their electromagnetic fields are localized at the interfaces and decay exponentially from the interfaces in the direction perpendicular to the interfaces. Therefore, we find (neglecting retardation effects) with the boundary condition $\boldsymbol{E}(\boldsymbol{q}_{||}, z)|_{z=\pm\infty} = 0$ from Maxwell's equations for the longitudinal part of the electric field

$$E_{||\mathrm{I}}^s(\boldsymbol{q}_{||}, z) = iC_{\mathrm{I}}^s \begin{cases} D_0^s\, \mathrm{e}^{-q_{||}(z-a)}; & z > a\,, \\ [A_1^s\, \mathrm{e}^{q_{||}z} - B_1^s\, \mathrm{e}^{-q_{||}z}]; & a > z > 0\,, \\ D_2^s\, \mathrm{e}^{q_{||}z}; & 0 > z\,. \end{cases} \tag{19}$$

C_{I}^s is a normalization constant, I denotes interface phonons, and s is the index of the different interface phonon modes. To derive the dispersion relation for the interface phonons we make use of the boundary conditions for the fields. We require that $E_{||\mathrm{I}}^s(\boldsymbol{q}_{||}, z)$ and $\varepsilon_\nu(\omega)\, \mathrm{d}E_{||\mathrm{I}}^s(\boldsymbol{q}_{||}, z)/\mathrm{d}z$ are continuous across the interfaces at $z = 0$, a and obtain [16]

$$(\varepsilon_1 + \varepsilon_2)^2 - (\varepsilon_1 - \varepsilon_2)^2\, \gamma^2 = 0 \tag{20}$$

with

$$\gamma = \mathrm{e}^{-q_{||}a}\,. \tag{21}$$

For the field amplitudes in (19) we find

$$\begin{aligned} D_0^s &= -1\,, \\ A_1^s &= \frac{\varepsilon_2 - \varepsilon_1}{2\varepsilon_1}\gamma\,, \\ B_1^s &= \frac{\varepsilon_1 + \varepsilon_2}{2\varepsilon_1}\gamma^{-1}\,, \\ D_2^s &= \frac{\varepsilon_1 + \varepsilon_2}{\varepsilon_2 - \varepsilon_1}\gamma^{-1}\,. \end{aligned} \tag{22}$$

Due to the symmetry of the DHS the dispersion relation (20) of the interface phonons is split into two different ones, one for the so-called antisymmetric interface phonon modes and one for the symmetric interface phonon modes. For the *antisymmetric interface phonon modes* the dispersion is

$$\varepsilon_1(\omega) + \varepsilon_2(\omega)\frac{1-\gamma}{1+\gamma} = 0\,. \tag{23}$$

With the use of the lattice dielectric functions (15) the explicit dispersion relation follows:

$$\omega_{\mathrm{A}\pm}(\boldsymbol{q}_{\|}) = \left\{\frac{1}{2(\varepsilon_1^{\mathrm{A}} + \varepsilon_2^{\mathrm{A}})}\left(\varepsilon_1^{\mathrm{A}}(\omega_{\mathrm{L1}}^2 + \omega_{\mathrm{T2}}^2) + \varepsilon_2^{\mathrm{A}}(\omega_{\mathrm{L2}}^2 + \omega_{\mathrm{T1}}^2) \pm [(\varepsilon_1^{\mathrm{A}}(\omega_{\mathrm{L1}}^2 + \omega_{\mathrm{T2}}^2) + \right.\right.$$

$$\left.\left. + \varepsilon_2^{\mathrm{A}}(\omega_{\mathrm{L2}}^2 + \omega_{\mathrm{T1}}^2))^2 - 4(\varepsilon_1^{\mathrm{A}} + \varepsilon_2^{\mathrm{A}})(\varepsilon_1^{\mathrm{A}}\omega_{\mathrm{L1}}^2\omega_{\mathrm{T2}}^2 + \varepsilon_2^{\mathrm{A}}\omega_{\mathrm{L2}}^2\omega_{\mathrm{T1}}^2)]^{1/2}\right\}^{1/2} \tag{24}$$

with

$$\varepsilon_1^{\mathrm{A}} = \varepsilon_{\infty 1}(1+\gamma)\,, \tag{25}$$

$$\varepsilon_2^{\mathrm{A}} = \varepsilon_{\infty 2}(1-\gamma)\,. \tag{26}$$

For the field amplitudes (22) we find for the antisymmetric interface phonon modes

$$\begin{aligned} D_0^{\mathrm{A}} &= -1\,, \\ A_1^{\mathrm{A}} &= -\frac{\gamma}{1-\gamma}\,, \\ B_1^{\mathrm{A}} &= -\frac{1}{1-\gamma}\,, \\ D_2^{\mathrm{A}} &= 1\,, \end{aligned} \tag{27}$$

and for the normalization constant according to (16)

$$C_1^{\mathrm{A}\pm} = \left\{\frac{q_{\|}(1-\gamma)}{2\varepsilon_0^2} \times \right.$$

$$\left. \times \left(\frac{(\omega_{\mathrm{T1}}^2 - \omega_{\mathrm{A}\pm}^2(\boldsymbol{q}_{\|}))^2(\omega_{\mathrm{T2}}^2 - \omega_{\mathrm{A}\pm}^2(\boldsymbol{q}_{\|}))^2}{\varepsilon_1^{\mathrm{A}}(\omega_{\mathrm{L1}}^2 - \omega_{\mathrm{T1}}^2)(\omega_{\mathrm{T2}}^2 - \omega_{\mathrm{A}\pm}^2(\boldsymbol{q}_{\|}))^2 + \varepsilon_2^{\mathrm{A}}(\omega_{\mathrm{L2}}^2 - \omega_{\mathrm{T2}}^2)(\omega_{\mathrm{T1}}^2 - \omega_{\mathrm{A}\pm}^2(\boldsymbol{q}_{\|}))^2}\right)\right\}^{1/2}. \tag{28}$$

The coupling function of a single electron with the antisymmetric interface phonons of the DHS is obtained from (13), (19) and (24) to (28),

$$\Gamma_{\mathrm{I}}^{\mathrm{A}\pm}(\boldsymbol{q}_{\|}, z) = -\left(\frac{\varepsilon_0 e^2 \hbar}{2A\omega_{\mathrm{A}\pm}(\boldsymbol{q}_{\|})}\right)^{1/2} \frac{C_{\mathrm{I}}^{\mathrm{A}\pm}}{q_{\|}} \times$$

$$\times \begin{cases} \mathrm{e}^{-q_{\|}(z-a)}; & z > a\,, \\ \dfrac{1}{1-\gamma}\left[\gamma\, \mathrm{e}^{q_{\|}z} - \mathrm{e}^{-q_{\|}z}\right]; & a > z > 0\,, \\ -\,\mathrm{e}^{q_{\|}z}; & 0 > z\,. \end{cases} \tag{29}$$

The implicit dispersion relation (20) contains also the dispersion relation for the *symmetric interface phonons*. Their dispersion relation is found from (20) to be

$$\varepsilon_1(\omega) + \varepsilon_2(\omega)\frac{1+\gamma}{1-\gamma} = 0\,. \tag{30}$$

With the use of the lattice dielectric functions (15) the explicit dispersion relation follows:

$$\omega_{\mathrm{S}\pm}(\boldsymbol{q}_{\|}) = \Big\{\frac{1}{2(\varepsilon_1^{\mathrm{S}} + \varepsilon_2^{\mathrm{S}})}\left(\varepsilon_1^{\mathrm{S}}(\omega_{\mathrm{L}1}^2 + \omega_{\mathrm{T}2}^2) + \varepsilon_2^{\mathrm{S}}(\omega_{\mathrm{L}2}^2 + \omega_{\mathrm{T}1}^2) \pm\right.$$

$$\pm \left[\left(\varepsilon_1^{\mathrm{S}}(\omega_{\mathrm{L}1}^2 + \omega_{\mathrm{T}2}^2) + \varepsilon_2^{\mathrm{S}}(\omega_{\mathrm{L}2}^2 + \omega_{\mathrm{T}1}^2)\right)^2 -\right.$$

$$\left.\left. - 4(\varepsilon_1^{\mathrm{S}} + \varepsilon_2^{\mathrm{S}})\left(\varepsilon_1^{\mathrm{S}}\omega_{\mathrm{L}1}^2\omega_{\mathrm{T}2}^2 + \varepsilon_2^{\mathrm{S}}\omega_{\mathrm{L}2}^2\omega_{\mathrm{T}1}^2\right)\right]^{1/2}\right)\Big\}^{1/2} \tag{31}$$

with

$$\varepsilon_1^{\mathrm{S}} = \varepsilon_{\infty 1}(1-\gamma)\,, \tag{32}$$

$$\varepsilon_2^{\mathrm{S}} = \varepsilon_{\infty 2}(1+\gamma)\,. \tag{33}$$

For the field amplitudes (22) we find for the symmetric interface phonon modes

$$\begin{aligned} D_0^{\mathrm{S}} &= -1\,, \\ A_1^{\mathrm{S}} &= -\frac{\gamma}{1+\gamma}\,, \\ B_1^{\mathrm{S}} &= \frac{1}{1+\gamma}\,, \\ D_2^{\mathrm{S}} &= -1\,, \end{aligned} \tag{34}$$

and for the normalization constant according to (16),

$$C_{\mathrm{I}}^{\mathrm{S}\pm} = \left\{\frac{q_{\|}(1+\gamma)}{2\varepsilon_0^2} \times \right.$$

$$\left. \times \left(\frac{\left(\omega_{\mathrm{T}1}^2 - \omega_{\mathrm{S}\pm}^2(\boldsymbol{q}_{\|})\right)^2\left(\omega_{\mathrm{T}2}^2 - \omega_{\mathrm{S}\pm}^2(\boldsymbol{q}_{\|})\right)^2}{\varepsilon_1^{\mathrm{S}}(\omega_{\mathrm{L}1}^2 - \omega_{\mathrm{T}1}^2)\left(\omega_{\mathrm{T}2}^2 - \omega_{\mathrm{S}\pm}^2(\boldsymbol{q}_{\|})\right)^2 + \varepsilon_2^{\mathrm{S}}(\omega_{\mathrm{L}2}^2 - \omega_{\mathrm{T}2}^2)\left(\omega_{\mathrm{T}1}^2 - \omega_{\mathrm{S}\pm}^2(\boldsymbol{q}_{\|})\right)^2}\right)\right\}^{1/2}. \tag{35}$$

The coupling function of a single electron with the symmetric interface phonons of the DHS is obtained from (13), (19), (31) to (35),

$$\Gamma_{\mathrm{I}}^{\mathrm{S}\pm}(\boldsymbol{q}_{||}, z) = -\left(\frac{\varepsilon_0 e^2 \hbar}{2A\omega_{\mathrm{S}\pm}(\boldsymbol{q}_{||})}\right)^{1/2} \frac{C_{\mathrm{I}}^{\mathrm{S}\pm}}{q_{||}} \times$$

$$\times \begin{cases} \mathrm{e}^{-q_{||}(z-a)}; & z > a\,, \\ \dfrac{1}{1+\gamma}\left[\gamma\, \mathrm{e}^{q_{||}z} + \mathrm{e}^{-q_{||}z}\right]; & q > z > 0\,, \\ \mathrm{e}^{q_{||}z} & 0 > z\,. \end{cases} \tag{36}$$

For numerical work we have chosen a $Ga_{0.75}Al_{0.25}As$–GaAs–$Ga_{0.75}Al_{0.25}As$ DHS. We describe both media by the lattice dielectric function (15). In the case of the ternary mixed crystal $Ga_{1-x}Al_xAs$ the single-mode expression (15) is an approximation since the lattice vibration behaviour of such mixed crystals is a complicated one (see for instance [17]). The material constants [18, 19] for GaAs are taken to be

$$\varepsilon_{\infty 1} = 10.90\,, \qquad \omega_{\mathrm{L}1} = 5.496 \times 10^{13}\,\mathrm{s}^{-1}\,, \qquad \omega_{\mathrm{T}1} = 5.057 \times 10^{13}\,\mathrm{s}^{-1}$$

and for $Ga_{0.75}Al_{0.25}As$

$$\varepsilon_{\infty 2} = 10.22\,, \qquad \omega_{\mathrm{L}2} = 6.979 \times 10^{13}\,\mathrm{s}^{-1} \quad \text{and} \quad \omega_{\mathrm{T}2} = 6.731 \times 10^{13}\,\mathrm{s}^{-1}\,.$$

In Fig. 3 the dispersion curves of the long-wave optical interface phonons are plotted. The dispersion curves start at $q_{||} = 0$ and $\omega = \omega_{\mathrm{T}1}$, $\omega_{\mathrm{L}1}$, $\omega_{\mathrm{T}2}$, or $\omega_{\mathrm{L}2}$, respectively. It is seen that the (+) modes approach the asymptotic frequency $\omega_{\mathrm{I}+}$ and the (−) modes approach $\omega_{\mathrm{I}-}$, respectively. These frequencies follow for $q_{||} \to \infty$ from (24) and (31). Fig. 4 shows the spatial dependence of the coupling function $\Gamma_{\mathrm{I}}^{s}(\boldsymbol{q}_{||}, z)$ (for $s = \mathrm{A}+, \mathrm{A}-, \mathrm{S}+, \mathrm{S}-$) of a single electron interacting with the four interface phonon modes. Since the media are isotropic in the x–y plane $\Gamma_{\mathrm{I}}^{s}(\boldsymbol{q}_{||}, z)$ is only a function of $q_{||} = |\boldsymbol{q}_{||}|$ and not of the direction of $\boldsymbol{q}_{||}$. The coupling function of the electron–interface phonon interaction is mainly localized at the interface of the DHS. Furthermore an interaction takes place even if the electron is outside the GaAs layer. Fig. 4 illustrates the spatial symmetry behaviour in z-direction of the four different interface modes. The (+) modes occur in the reststrahlen branch of $Ga_{1-x}Al_xAs$, the (−) modes in that of GaAs. Therefore, the (−) modes which are supported by the GaAs layer would also occur in a free standing GaAs layer. In such a case, an electron outside the GaAs layer in the vacuum interacts also with the (−) interface phonon modes. This effect is used in EELS measurements. From (29) and (36) it is to be seen that the

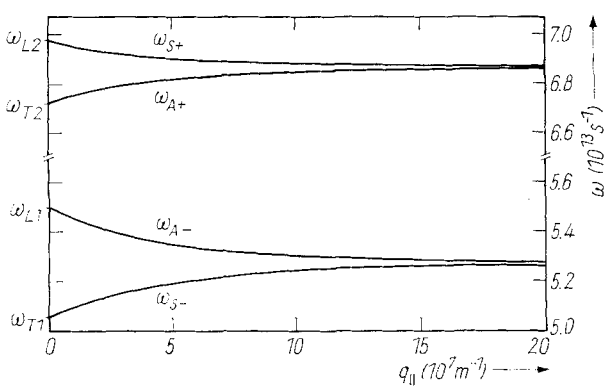

Fig. 3. Dispersion relation of long-wave optical interface phonons of a GaAs–$Ga_{0.75}Al_{0.25}As$ DHS for a thickness of $a = 20$ nm of the GaAs layer

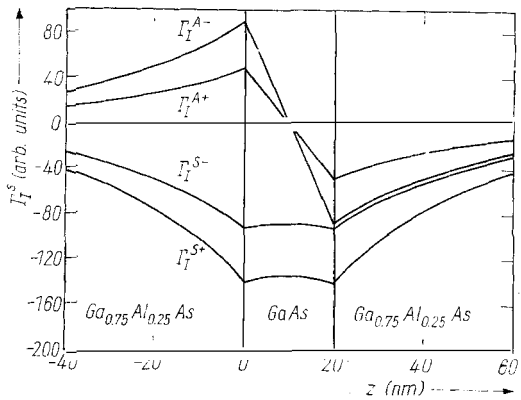

Fig. 4. Spatial dependence of the coupling function $\Gamma_{\mathrm{I}}^{s}(q_{\|}, z)$ of the electron–(long-wave optical) interface phonon interaction of a GaAs–$Ga_{0.75}Al_{0.25}As$ DHS for a thickness of $a = 20$ nm of the GaAs layer and $q_{\|} = 3 \times 10^7$ cm^{-1}

localization of the coupling function $\Gamma_{\mathrm{I}}^{s}(\boldsymbol{q}_{\|}, z)$ for the interface phonon modes increases with larger values of the wave vector component $q_{\|}$.

3.2 LO phonons

Besides the interface phonons there exist also the bulk-like LO phonons in the spectrum of the long-wave optical phonons. The LO phonons only occur at those frequencies where the lattice dielectric functions of the semiconductors forming the individual layers of the DHS vanish. With the lattice dielectric function (15) the frequency of each longitudinal layer resonance is identical to that of the relevant bulk LO phonon. But other properties, such as the spatial dependence of the electric field strength, will be altered due to the existence of the interfaces. From Maxwell's equations and boundary conditions for the field components across the interfaces of the DHS it is found that the electric field of the LO phonons ω_{L1} is only different from zero inside the layer (1) and that of the LO phonons ω_{L2} is only different from zero in the surrounding medium (2) [15]. Simple calculations result in the coupling function of a single electron with the LO phonon modes ω_{L1} of medium 1

$$\Gamma_{\mathrm{L1}}^{m}(\boldsymbol{q}_{\|}, z) = -\left(\frac{e^2\hbar\omega_{\mathrm{L1}}}{Aa\varepsilon_0}\left(\frac{1}{\varepsilon_{\infty 1}} - \frac{1}{\varepsilon_{s1}}\right)\right)^{1/2} \begin{cases} 0; & z > a, \\ \dfrac{\sin(q_1^m z)}{\sqrt{q_{\|}^2 + (q_1^m)^2}}; & a > z > 0, \\ 0; & 0 > z, \end{cases} \tag{37}$$

with

$$q_1^m = \frac{\pi}{a} m; \qquad m = 1, 2, 3, \ldots . \tag{38}$$

Herein $\varepsilon_{s\nu} = \varepsilon_{\infty\nu}(\omega_{\mathrm{L}\nu}/\omega_{\mathrm{T}\nu})^2$ denotes the static dielectric constant. The coupling function of a single electron with the LO phonon modes ω_{L2} of medium 2 is given by

$$\Gamma_{\mathrm{L2}}(\boldsymbol{q}_{\|}, q_z, z) = -\left(\frac{e^2\hbar\omega_{\mathrm{L2}}}{V_{\mathrm{G}}\varepsilon_0}\left(\frac{1}{\varepsilon_{\infty 2}} - \frac{1}{\varepsilon_{s2}}\right)\right)^{1/2} \times$$
$$\times \begin{cases} \dfrac{\sin\left(q_z(z-a)\right)}{\sqrt{q_{\|}^2 + q_z^2}}; & z > a, \\ 0; & a > z > 0, \\ \dfrac{\sin(q_z z)}{\sqrt{q_{\|}^2 + q_z^2}}; & 0 > z, \end{cases} \tag{39}$$

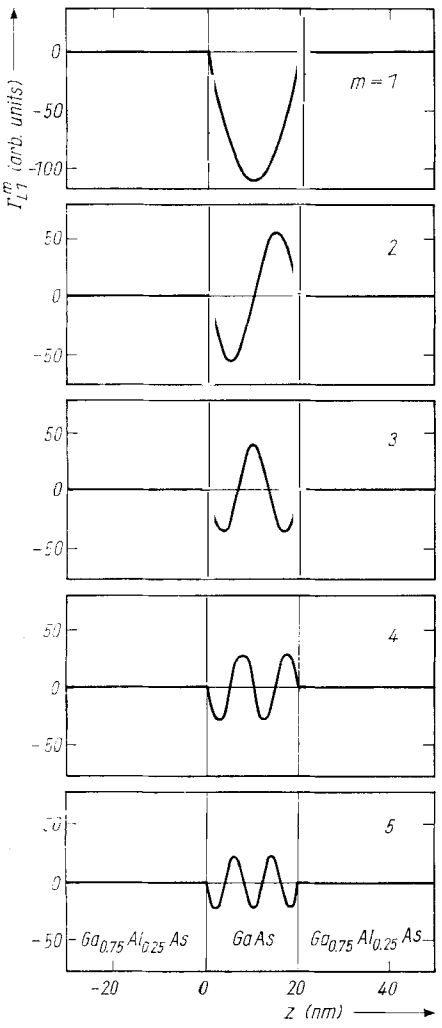

Fig. 5. Spatial dependence of the coupling function $\Gamma^m_{L1}/(q_{||}, z)$ of the electron–LO phonon interaction of a GaAs–$Ga_{0.75}Al_{0.25}As$ DHS for $a = 20$ nm and $q_{||} = 3 \times 10^7$ m^{-1}

with V_G the unit volume and q_z the z-component of the three-dimensional wave vector $\boldsymbol{q}$. The LO phonons of media 1/2 are composed of ordinary bulk LO phonons which propagate to the interfaces of the DHS and are backscattered from them. At the interfaces of the DHS itself, i.e. at $z = 0$ and $z = a$, the influence of these modes vanishes due to the interference of incident and backscattered waves. This is the physical reason for the discreteness of the z-component of the wave vector $\boldsymbol{q}$ of the LO phonons of the layer (1). According to the discussion above, Γ_{L2} is identical to the well-known Fröhlich coupling in the 3D bulk case [20] if we neglect the backscattered part. Their is an important difference between the Fröhlich coupling of confined LO phonons in layered systems and of ordinary 3D LO phonons. Whereas the 3D phonon wave vector of the 3D bulk LO phonons starts at $|\boldsymbol{q}| = 0$, for the confined LO phonons of a semiconductor layer wave vectors smaller than $|\boldsymbol{q}| = \pi/a$ are forbidden. In Fig. 5 we have plotted the spatial dependence of the coupling function $\Gamma^m_{L1}(\boldsymbol{q}_{||}, z)$ of a single electron interacting with the LO phonon modes ω_{L1} of the GaAs layer. It is to be seen that the interaction strength vanishes outside the GaAs layer and at the interfaces.

4. The Screened Potential

Up to now we have considered the interaction of a single electron with the different kinds of long-wave optical phonons of the DHS. The important quantity $\Gamma_j(\boldsymbol{q}_{||}, z)$ describes the coupling strength of the different long-wave optical phonons to the charge of the single electron at the position z. This is the theory for a DHS equivalent to the well-known Fröhlich polaron in three dimensions. But in the case of a DHS the electrons form a Q2DEG. Therefore, we must investigate a many-electron problem in a layered structure where the electrons interact with the different kinds of long-wave optical phonons. To solve this problem we have to calculate the longitudinal, dynamically screened interaction potential of an electron with another one. In [11] we have derived the Dyson equation for this screened interaction potential in the "subband space". It reads

$$W^{sc}_{K_1K_2K_3K_4}(\boldsymbol{q}_{||}, \omega) = W_{K_1K_2K_3K_4}(\boldsymbol{q}_{||}, \omega) + \sum_{LL'} W_{K_1K_2L'L}(\boldsymbol{q}_{||}, \omega)\, P^{(1)}_{LL'}(\boldsymbol{q}_{||}, \omega)\, W^{sc}_{LL'K_3K_4}(\boldsymbol{q}_{||}, \omega)\,. \quad (40)$$

In this equation the bare interaction potential is given by

$$W_{K_1K_2K_3K_4}(\boldsymbol{q}_{||}, \omega) = V^{\infty}_{K_1K_2K_3K_4}(\boldsymbol{q}_{||}) + V^{\mathrm{ph}}_{K_1K_2K_3K_4}(\boldsymbol{q}_{||}, \omega) , \tag{41}$$

where $V^{\infty}_{K_1K_2K_3K_4}(\boldsymbol{q}_{||})$ represents the bare electron–electron interaction (bare or direct Coulomb) and $V^{\mathrm{ph}}_{K_1K_2K_3K_4}(\boldsymbol{q}_{||}, \omega)$ the bare electron–phonon interaction. The bare electron–electron interaction potential is given by

$$V^{\infty}_{K_1K_2K_3K_4}(\boldsymbol{q}_{||}) = \frac{e^2}{2\varepsilon_0\varepsilon_{\infty 1} q_{||}} f^{C}_{K_1K_2K_3K_4}(\boldsymbol{q}_{||}) \tag{42}$$

with the form factor

$$f^{\mathrm{C}}_{K_1K_2K_3K_4}(\boldsymbol{q}_{||}) = \int \mathrm{d}z \int \mathrm{d}z' \, \varphi^{*}_{K_1}(z) \, \varphi_{K_2}(z) \, \mathrm{e}^{-q_{||}|z-z'|} \, \varphi^{*}_{K_3}(z') \, \varphi_{K_4}(z') . \tag{43}$$

The electron–electron interaction potential contains the optical dielectric constant $\varepsilon_{\infty 1}$ of that semiconductor containing the Q2DEG. The factor $\varepsilon_{\infty 1}$ includes the dielectric screening of the semiconductor background arising from high-energy electronic excitations across the band gap. The bare electron–phonon interaction potential is given by

$$V^{\mathrm{ph}}_{K_1K_2K_3K_4}(\boldsymbol{q}_{||}, \omega) = \frac{2}{\hbar} \sum_{j} \frac{\omega_j(\boldsymbol{q}_{||})}{(\omega + i\delta)^2 - \omega_j^2(\boldsymbol{q}_{||})} f^{j}_{K_1K_2K_3K_4}(\boldsymbol{q}_{||}) \tag{44}$$

with

$$f^{j}_{K_1K_2K_3K_4}(\boldsymbol{q}_{||}) = M^{j}_{K_1K_2}(\boldsymbol{q}_{||}) \, M^{j}_{K_3K_4}(-\boldsymbol{q}_{||}) . \tag{45}$$

Throughout this paper we only use *retarded* functions ($\delta \to 0^{+}$). The basic electron–phonon interaction vertex is represented by the matrix element $M^{j}_{K'K}(\boldsymbol{q}_{||})$ of the coupling function $\Gamma_j(\boldsymbol{q}_{||}, z)$ with the envelope wave function according to

$$M^{j}_{K'K}(\boldsymbol{q}_{||}) = \sqrt{A} \int \mathrm{d}z \, \varphi^{*}_{K'}(z) \, \Gamma_j(\boldsymbol{q}_{||}, z) \, \varphi_K(z) . \tag{46}$$

Therefore this vertex includes the spatial dependence of the envelope wave function of the scattered electron ($K \to K'$) in distinction to the coupling function $\Gamma_j(\boldsymbol{q}_{||}, z)$. Within the random-phase approximation [21, 22] the polarization function $P^{(1)}_{KK'}(\boldsymbol{q}_{||}, \omega)$ is

$$P^{(1)}_{KK'}(\boldsymbol{q}_{||}, \omega) = \frac{2}{A} \sum_{\boldsymbol{k}_{||}} \frac{n_{\mathrm{F}}\big(\xi_{K'}(\boldsymbol{k}_{||})\big) - n_{\mathrm{F}}\big(\xi_K(\boldsymbol{k}_{||} + \boldsymbol{q}_{||})\big)}{(\hbar\omega + i\delta) + \xi_{K'}(\boldsymbol{k}_{||}) - \xi_K(\boldsymbol{k}_{||} + \boldsymbol{q}_{||})} \tag{47}$$

with the Fermi occupancy factor n_{F} and $\xi_K(\boldsymbol{k}_{||}) = \mathscr{E}_K(\boldsymbol{k}_{||}) - \mu$. The dynamically screened and finite-temperature interaction potential (40) contains all the information needed in order to derive the dispersion relation of the collective excitations of the DHS. But in general, it is quite difficult to obtain it exactly from (40). Therefore, two approximations are made in the Dyson equation. At first we take into account the assumption of the electric quantum limit. This means that only the lowest subband is occupied. In that case we put $K_2 = K_4 = 0$ and define

$$\chi^{(1)}_K(\boldsymbol{q}_{||}, \omega) = \begin{cases} P^{(1)}_{00}(\boldsymbol{q}_{||}, \omega) & \text{if} \quad K = 0 , \\ P^{(1)}_{K0}(\boldsymbol{q}_{||}, \omega) + P^{(1)}_{0K}(\boldsymbol{q}_{||}, \omega) & \text{if} \quad K > 0 . \end{cases} \tag{48}$$

The full RPA expression of the polarization function $\chi^{(1)}_K(\boldsymbol{q}_{||}, \omega)$ of a Q2DEG in the zero-temperature limit was calculated by Wendler and Pechstedt [11].

For the subband indices we write for simplicity $\{K_1 0 K_3 0\} \equiv \{K_1 K_3\}$. As a further approximation we neglect the off-diagonal elements of (40). The form factors f^{C}_{KK} (43) and f^{L1}_{KK}, $f^{\mathrm{A}\pm}_{KK}$ and $f^{\mathrm{S}\pm}_{KK}$ (45) are easily calculated for a DHS. For the form factor of the

bare electron–electron interaction (43) follows with (7)

$$f^{\mathrm{C}}_{KK}(\boldsymbol{q}_{||}) = (q_{||}a)\left[\frac{1}{(q_{||}a)^2 + \pi^2(K+2)^2} + \frac{1 + \delta_{K0}}{(q_{||}a)^2 + (\pi K)^2}\right] -$$
$$- 2(q_{||}a)^2\,[1 - (-1)^K\,\gamma]\left\{\frac{(2\pi)^2\,(K+1)}{\left((q_{||}a)^2 + (\pi K)^2\right)\left((q_{||}a)^2 + \pi^2(K+2)^2\right)}\right\}^2. \quad (49)$$

In Fig. 6 we have plotted $f^{\mathrm{C}}_{KK}(\boldsymbol{q}_{||})$ for (0–0) intrasubband scattering ($K = 0$) and for (1–0) intersubband scattering ($K = 1$). It is to be seen that in a wide range of $q_{||}$, $f^{\mathrm{C}}_{11}(\boldsymbol{q}_{||})$ is smaller than $f^{\mathrm{C}}_{00}(\boldsymbol{q}_{||})$. Discussing the bare electron–phonon interaction we give at first the result for the matrix elements $M^{j}_{K0}(\boldsymbol{q}_{||})$. For the matrix element of the interface phonons of the DHS it follows:

$$M^{\mathrm{A}\pm}_{K0}(\boldsymbol{q}_{||}) = -\left(\frac{\varepsilon_0 e^2\hbar}{2\omega_{\mathrm{A}\pm}(\boldsymbol{q}_{||})}\right)^{1/2}\frac{C^{\mathrm{A}\pm}_{\mathrm{I}}}{1-\gamma}\,[1+\gamma]\,(1-(-1)^K)\times$$
$$\times\left[\frac{a}{(q_{||}a)^2 + \pi^2(K+2)^2} - \frac{a}{(q_{||}a)^2 + (\pi K)^2}\right] \quad (50)$$

and

$$M^{\mathrm{S}\pm}_{K0}(\boldsymbol{q}_{||}) = \left(\frac{\varepsilon_0 e^2\hbar}{2\omega_{\mathrm{S}\pm}(\boldsymbol{q}_{||})}\right)^{1/2}\frac{C^{\mathrm{S}\pm}_{\mathrm{I}}}{1+\gamma}\,[1-\gamma]\,(1+(-1)^K)\times$$
$$\times\left[\frac{a}{(q_{||}a)^2 + \pi^2(K+2)^2} - \frac{a}{(q_{||}a)^2 + (\pi K)^2}\right] \quad (51)$$

and for the matrix element of the LO phonons of the DHS (modes of the GaAs layer):

$$M^{\mathrm{L1},m}_{K0}(\boldsymbol{q}_{||}) = \begin{cases} \left(\dfrac{e^2\hbar\omega_{\mathrm{L1}}}{a\varepsilon_0}\left(\dfrac{1}{\varepsilon_{\infty 1}} - \dfrac{1}{\varepsilon_{\mathrm{s}1}}\right)\right)^{1/2}\dfrac{1}{\sqrt{q_{||}^2 + (q_1^m)^2}}\,\dfrac{4m(K+1)\,(1-(-1)^{K+m})}{\pi(K^2-m^2)\,((K+2)^2-m^2)}; \\ 0; \\ \text{if} \quad K \neq m \quad \text{and} \quad K+2 \neq m \\ \text{if} \quad K = m \quad \text{and} \quad K+2 = m \end{cases} \quad (52)$$

Due to the symmetry of the DHS only the symmetric interface phonon modes and the LO phonon modes $m = 1, 3, 5, \ldots$ cause the (0–0) intrasubband scattering and only the antisymmetric interface phonon modes and the LO phonon modes $m = 2, 4, 6, \ldots$ cause the (1–0) intersubband scattering. A similar result was obtained in [23]. It is to be seen from (52) that the interaction strength with the LO phonons decreases with increasing mode index m. According to (45) and (50), (51) $f^{\mathrm{A}\pm}_{KK}(\boldsymbol{q}_{||})$ and $f^{\mathrm{S}\pm}_{KK}(\boldsymbol{q}_{||})$ are given by the square of $M^{\mathrm{A}\pm}_{K0}(\boldsymbol{q}_{||})$ and $M^{\mathrm{S}\pm}_{K0}(\boldsymbol{q}_{||})$, respectively. For the form

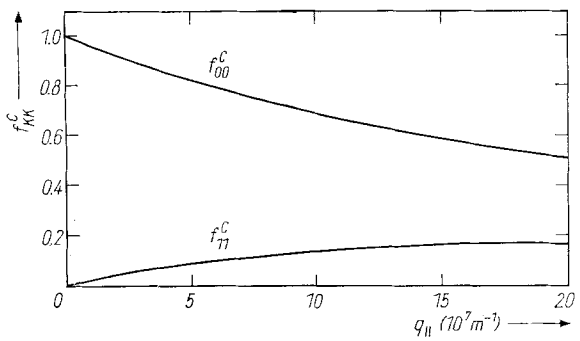

Fig. 6. Form factors $f^{\mathrm{C}}_{00}(q_{||})$ and $f^{\mathrm{C}}_{11}(q_{||})$ of the electron–electron interaction of a GaAs–$Ga_{0.75}Al_{0.25}As$ DHS for $a =$ = 20 nm

factor of the LO phonons we define

$$f_{KK}^{\mathrm{L1}}(\boldsymbol{q}_{||}) = \sum_{m=1}^{\infty} M_{K0}^{\mathrm{L1},m}(\boldsymbol{q}_{||})\, M_{K0}^{\mathrm{L1},m}(-\boldsymbol{q}_{||})\,, \tag{53}$$

where we perform the sum over m before integrating. The sum over m in (53) may be converted to an integral and the result evaluated to give

$$\begin{aligned} f_{KK}^{\mathrm{L1}}(\boldsymbol{q}_{||}) = {} & \frac{e^2\hbar\omega_{\mathrm{L1}}}{4\varepsilon_0 q_{||}}\left(\frac{1}{\varepsilon_{\infty 1}}-\frac{1}{\varepsilon_{\mathrm{s}1}}\right)\left\{(q_{||}a)\left[\frac{1}{(q_{||}a)^2+\pi^2(K+2)^2}+\frac{1+\delta_{K0}}{(q_{||}a)^2+(\pi K)^2}\right]-\right. \\ & -(q_{||}a)^2\left[1-(-1)^K\gamma\right]\left[3-(-1)^K\gamma\right]\times \\ & \left.\times\left[\frac{(2\pi)^2(K+1)}{\left((q_{||}a)^2+(\pi K)^2\right)\left((q_{||}a)^2+\pi^2(K+2)^2\right)}\right]^2\right\}. \end{aligned} \tag{54}$$

In many papers dealing with the same subject only the interaction of a strict 2DEG with the bulk LO phonons is considered, neglecting any effect of the interface. To compare the form factors $f_{KK}^{\mathrm{A}\pm}(\boldsymbol{q}_{||})$, $f_{KK}^{\mathrm{S}\pm}(\boldsymbol{q}_{||})$ and $f_{KK}^{\mathrm{L1}}(\boldsymbol{q}_{||})$ of the present paper with such a form factor we will derive them. The starting point is the Fröhlich polaron Hamiltonian which contains the coupling function (39) if we neglect the backscattered wave. Performing the sum over q_z (may be converted to an integral) and using for the envelope wave function of the strict 2DEG $|\varphi(z)|^2 = \delta(z)$ it follows:

$$f^{\mathrm{LO}}(\boldsymbol{q}_{||}) = \frac{e^2\hbar\omega_{\mathrm{L1}}}{4\varepsilon_0 q_{||}}\left(\frac{1}{\varepsilon_{\infty 1}}-\frac{1}{\varepsilon_{\mathrm{s}1}}\right). \tag{55}$$

In Fig. 7a the form factors $f_{00}^{\mathrm{S}\pm}(\boldsymbol{q}_{||})$ and $f_{00}^{\mathrm{L1}}(\boldsymbol{q}_{||})$ are plotted and in Fig. 7b $f_{11}^{\mathrm{A}\pm}(\boldsymbol{q}_{||})$ and $f_{11}^{\mathrm{L1}}(\boldsymbol{q}_{||})$. Since these form factors represent the strength of the scattering process of two electrons of the lowest subband, Fig. 7 a, b show at each value of the wave vector component $q_{||}$ which is the dominant interaction process. Especially at low values of $q_{||}$ the dominant interaction for the (0–0) intersubband scattering is that with the S+-interface phonon mode. At large wave vectors the dominant scattering arises always from the interaction with the LO phonons.

5. Collective Excitations

The Dyson equation (40) for the screened interaction potential provides the definition of the total longitudinal dielectric function of the DHS. Using the two approximations described above the total longitudinal dielectric function is given by

$$\varepsilon_{KK}^{\mathrm{total}}(\boldsymbol{q}_{||},\omega) = V_{KK}^{\mathrm{C}}(\boldsymbol{q}_{||})\left(W_{KK}^{-1}(\boldsymbol{q}_{||},\omega) - \chi_K^{(1)}(\boldsymbol{q}_{||},\omega)\right) \tag{56}$$

with $V_{KK}^{\mathrm{C}}(\boldsymbol{q}_{||}) = \varepsilon_{\infty 1} V_{KK}^{\infty}(\boldsymbol{q}_{||})$. This dielectric function of the DHS is responsible for a variety of excitations of the polaron gas including the different kinds of long-wave optical phonons and their coupling to the charge-density excitations of the Q2DEG. In the regions of the $\omega - q_{||}$ plane with $\mathrm{Im}\,\varepsilon_{KK}^{\mathrm{total}}(\boldsymbol{q}_{||},\omega) = 0$ the dispersion relation of the coupled excitations follows from $\mathrm{Re}\,\varepsilon_{KK}^{\mathrm{total}}(\boldsymbol{q}_{||},\omega) = 0$:

$$W_{KK}^{-1}(\boldsymbol{q}_{||},\omega) - \chi_K^{(1)}(\boldsymbol{q}_{||},\omega) = 0\,. \tag{57}$$

Since the dispersion relation contains long-wave optical phonons (both interface and LO phonons) as well as charge-density excitations of the Q2DEG, it describes

(i) coupled intrasubband plasmon–phonon modes if $K = 0$ and
(ii) coupled intersubband plasmon–phonon modes if $K > 0$.

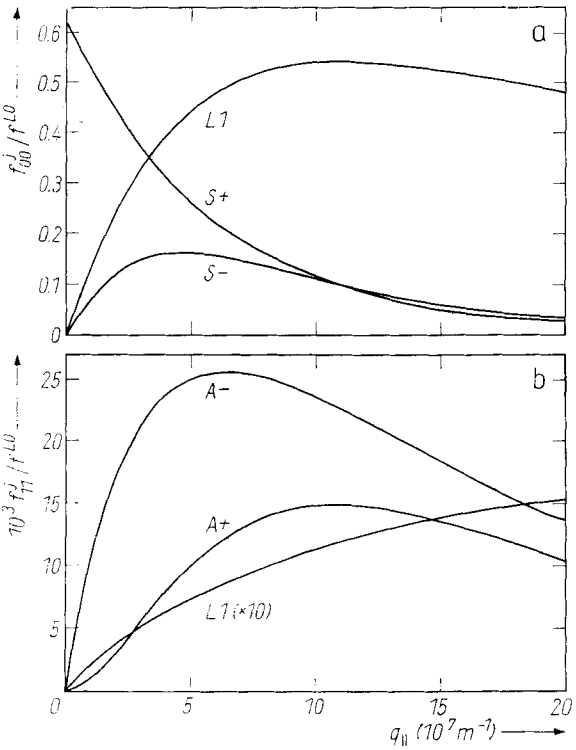

Fig. 7. Plot of the form factors $f^j_{KK}(q_{||})$ (normalized to the form factor $f^{L0}(q_{||})$) of a GaAs–$Ga_{0.75}Al_{0.25}As$ DHS for $a = 20$ nm. a) $f^{S\pm}_{00}/f^{L0}$ and f^{L1}_{00}/f^{L0}; b) $f^{A\pm}_{11}/f^{L0}$ and f^{L1}_{11}/f^{L0}. (The values of curve L1 have to be multiplicated by a factor of 10)

From the dispersion relation it can be seen that the neglect of the off-diagonal elements of the Dyson equation is equivalent to neglecting the mixing between intra- and intersubband and between different intersubband excitations.

The full RPA excitation spectrum of a Q2DEG, which is determined by (57) and (48) with $V^{ph}_{KK}(\boldsymbol{q}_{||}, \omega) = 0$, is plotted in Fig. 8. The excitations can be separated in *collective intrasubband excitations*, *single-particle intrasubband excitations* (the (0–0) excitations are plotted) and in *collective intersubband excitations* and *single-particle intersubband excitations* (the (1–0) excitations are plotted). The collective excitations, intrasubband plasmons ω^{00}_p and intersubband plasmons ω^{10}_p, are solutions of (57), whereas the single-particle excitations form the continuous areas in the ω–$q_{||}$ plane. These regions in the ω–$q_{||}$ plane, in which $\mathrm{Im}\,\chi^{(1)}_K(\boldsymbol{q}_{||}, \omega)$ is nonzero, are shown in Fig. 8 by the shaded regions given by

$$v_F q_{||}\left(-1 + \frac{q_{||}}{2k_F}\right) + \Omega_{K0} < \omega < v_F q_{||}\left(1 + \frac{q_{||}}{2k_F}\right) + \Omega_{K0}\,. \tag{58}$$

$\hbar\Omega_{K0} = \mathscr{E}_K - \mathscr{E}_0$ denotes the subband separation, $k_F = (2\pi n_{2DEG})^{1/2}$ is the Fermi wave vector and $v_F = \hbar k_F/m$ the Fermi velocity. The collective excitations inside the single-particle continuum are Landau damped and (57) does not give the correct results. In such cases the collective excitations of the DHS can be obtained from the peaks of the energy-loss function which is proportional to $\mathrm{Im}\left(-1/\varepsilon^{total}_{KK}(\boldsymbol{q}_{||}, \omega)\right)$.

Only the collective excitations existing in the unshaded regions of Fig. 8 are not Landau damped and therefore they should have long life-times.

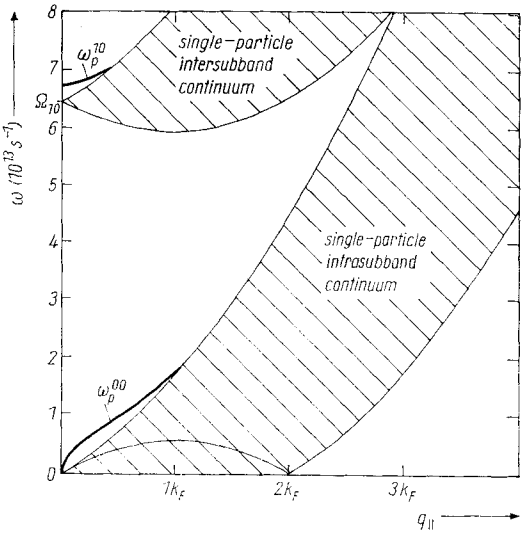

Fig. 8. Excitation spectrum of the Q2DEG in the ω–$q_{||}$ plane for $n_{2DEG} = 1 \times 10^{11}\ cm^{-2}$ ($k_F = 7.927 \times 10^7\ m^{-1}$) and $a = 20$ nm. The regions of the single-particle excitations are shown by the shaded regions and the dispersion curves of the intra- (0–0) and (1–0) intersubband collective excitations (calculated within the RPA) by heavy solid lines, respectively

5.1 Coupled intrasubband plasmon–phonons

The dispersion relation of the coupled intrasubband plasmon-phonons is given by (57) for $K = 0$. If we use (47) and (48) for the polarization function the full RPA spectrum is obtained [12]. For numerical work we have chosen a $Ga_{0.75}Al_{0.25}As$–GaAs–$Ga_{0.75}Al_{0.25}As$ DHS with the material parameters given in Section 3.1 and for the conduction band mass of GaAs [18] we use $m = 0.06624 m_0$. Fig. 9 a to d show the full RPA dispersion curves of the coupled intrasubband plasmon-phonon modes for different sheet carrier concentrations and different thicknesses of the GaAs layer. Due to the symmetry properties of the DHS the intrasubband plasmons couple only to the LO phonons of the GaAs layer and to the symmetric interface phonons, but not to the antisymmetric one. For high sheet carrier concentrations the dispersion curve of the uncoupled intrasubband plasmon mode ω_p^{00} crosses the dispersion curves of the uncoupled phonon modes ω_{L1} and $\omega_{S\pm}$ resulting in four *resonance split dispersion curves* of the coupled intrasubband plasmon-phonon modes. The coupled phonon-like modes start for $q_{||} = 0$ at the frequencies ω_{T1}, ω_{L1}, and ω_{L2} as the uncoupled modes, too. This behaviour differs from that in the 3D case [24]. The coupled plasmon-like mode starts for $q_{||} = 0$ at $\omega = 0$. For large values of $q_{||}$ the dispersion curves penetrate the single-particle intrasubband continuum. It is seen from Fig. 9 that the strength of the plasmon-phonon coupling increases with increasing sheet carrier concentration and decreases with increasing layer thickness a of the GaAs layer. But the influence of a thickness variation does not change the resulting intrasubband mode spectrum dramatically. The dependence on the sheet carrier concentration is much stronger. The dispersion curves plotted in Fig. 10 are calculated in RPA, in the plasmon-pol approximation (PPA), and in the long-wave approximation (LWA). The polarisation functions for the last two approximations are discussed in [11]. It is seen that for large values of $q_{||}$ the RPA results deviate appreciably from the PPA and LWA ones. These reason is that the PPA and LWA results are restricted to $q_{||} \ll \omega/v_F$ and the strong spatial dispersion included within RPA becomes important for large values of $q_{||}$. This more exact results of our RPA calculations should be in principle measurable in spectroscopic experiments on collective excitations in DHS's. The dispersion relation (57) contains a lot of special cases. If we expand $\chi_0^{(1)}(\boldsymbol{q}_{||}, \omega)$ in (48) to $O(q_{||}^4)$ neglecting

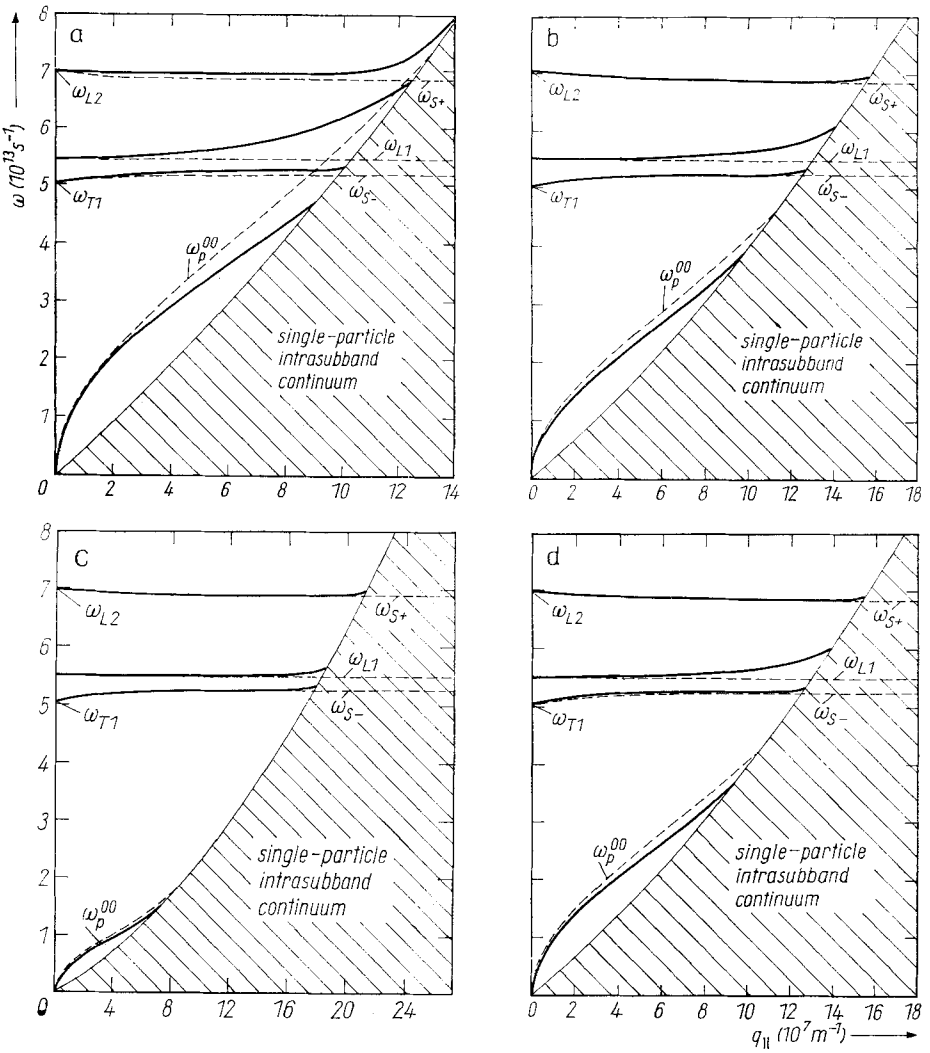

Fig. 9. Dispersion relation of the coupled intrasubband plasmon–phonons in RPA of the GaAs–$Ga_{0.75}Al_{0.25}As$ DHS (solid lines) for a) $n_{2DEG} = 1 \times 10^{12}$ cm^{-2}, $a = 20$ nm; b) $n_{2DEG} = 5 \times 10^{11}$ cm^{-2}, $a = 20$ nm; c) $n_{2DEG} = 1 \times 10^{11}$ cm^{-2}, $a = 20$ nm; and d) $n_{2DEG} = 5 \times 10^{11}$ cm^{-2}, $a = 25$ nm. The dispersion relation of the uncoupled modes is given by the dashed lines

the contribution from the long-wave optical phonons ($V_{00}^{ph}(\boldsymbol{q}_{||}, \omega) = 0$) and use $|\varphi(z)|^2 = \delta(z)$ in (43) the dispersion relation of 2D plasmons follows from (57) ([25]):

$$\omega = \sqrt{\omega_p^2 + \tfrac{3}{4} v_F^2 q_{||}^2}$$

with the 2D plasma frequency

$$\omega_p = \left(\frac{n_{2DEG} e^2}{2m\varepsilon_0 \varepsilon_{\infty 1}} q_{||} \right)^{1/2} . \tag{59}$$

Using the LWA approximation (expanding to $O(q_{||}^2)$) for $\chi_0^{(1)}(\boldsymbol{q}_{||}, \omega)$ the dispersion relation for the coupled excitation: strict 2D plasmon–3D LO phonon follows from

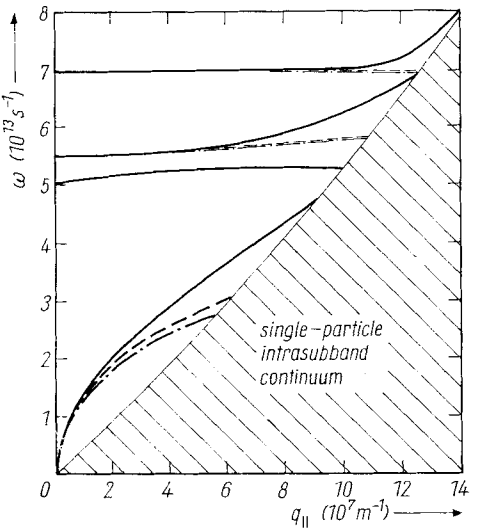

Fig. 10

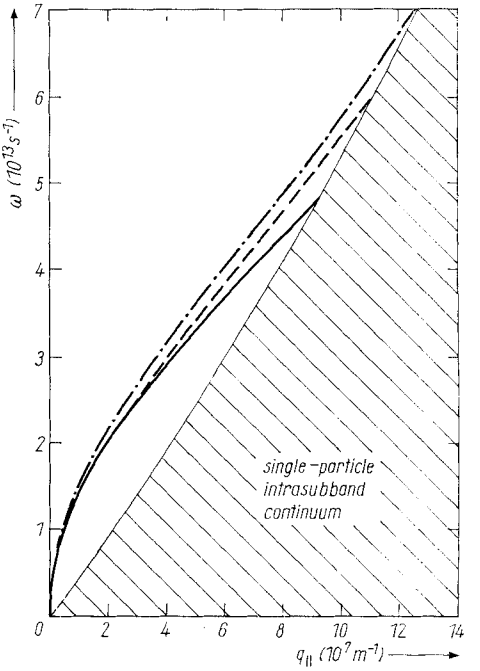

Fig. 11

Fig. 10. Dispersion relation of the coupled intrasubband plasmon–phonons in RPA (solid lines PPA (dashed lines), and LWA (dash-dotted lines) of the GaAs–$Ga_{0.75}Al_{0.25}As$ DHS for $n_{2DEG} = 1 \times 10^{12}$ cm^{-2}, $a = 20$ nm

Fig. 11. Dispersion relation of the intrasubband plasmon in RPA including the dynamical plasmon phonon coupling (solid line), in the ε_s-approximation (dashed line), and without any phonon contribution (dash-dotted line) of the GaAs–$Ga_{0.75}Al_{0.25}As$ DHS for $n_{2DEG} = 1 \times 10^{12}$ cm^{-2}, $a = 20$ nm

(57) with (55) [26]:

$$\omega_{\pm} = \{\tfrac{1}{2}((\omega_{L1}^2 + \omega_p^2) \pm [(\omega_{L1}^2 + \omega_p^2)^2 - 4\omega_{T1}^2\omega_p^2]^{1/2})\}^{1/2} . \tag{60}$$

This restrictive approximation is mostly used when dynamical phonon effects on the plasmons in quantum wells and superlattices are treated [3]. The result (60) can also be derived by neglecting the interaction potential $V_{00}^{ph}(\boldsymbol{q}_{||}, \omega) = 0$ but replacing $\varepsilon_{\infty 1}$ by $\varepsilon_1(\omega) = \varepsilon_{\infty 1}(\omega_{L1}^2 - \omega^2)/(\omega_{T1}^2 - \omega^2)$ in $V_{00}^{\infty}(q_{||})$ as done in [3]. If one omits the important effect of the interfaces, this results in the loss of dispersion curves in the spectrum of the collective excitations. Another approximation use dvery often, the ε_s-approximation for the phonon contribution of the DHS, neglects any dynamical phonon contribution in the dispersion relation (57). In this case the RPA dispersion relation of the Q2D intrasubband plasmons follows from (48) and (57) neglecting $V_{00}^{ph}(\boldsymbol{q}_{||}, \omega)$ and replacing $\varepsilon_{\infty 1}$ in (42) by ε_{s1}. In Fig. 11 we have plotted the dispersion curve of the plasmons including the dynamical phonon effect, the ε_s-approximation, and without any phonon contribution.

5.2 Coupled intersubband plasmon–phonons

In this section we discuss the (1–0) coupled intersubband plasmon–phonons. Their dispersion relation is given by (57) for $K = 1$. In Fig. 12 a to d we have plotted the

dispersion curves of the (1–0) coupled intersubband plasmon–phonon modes for different sheet carrier concentrations and different thicknesses of the GaAs layer. The

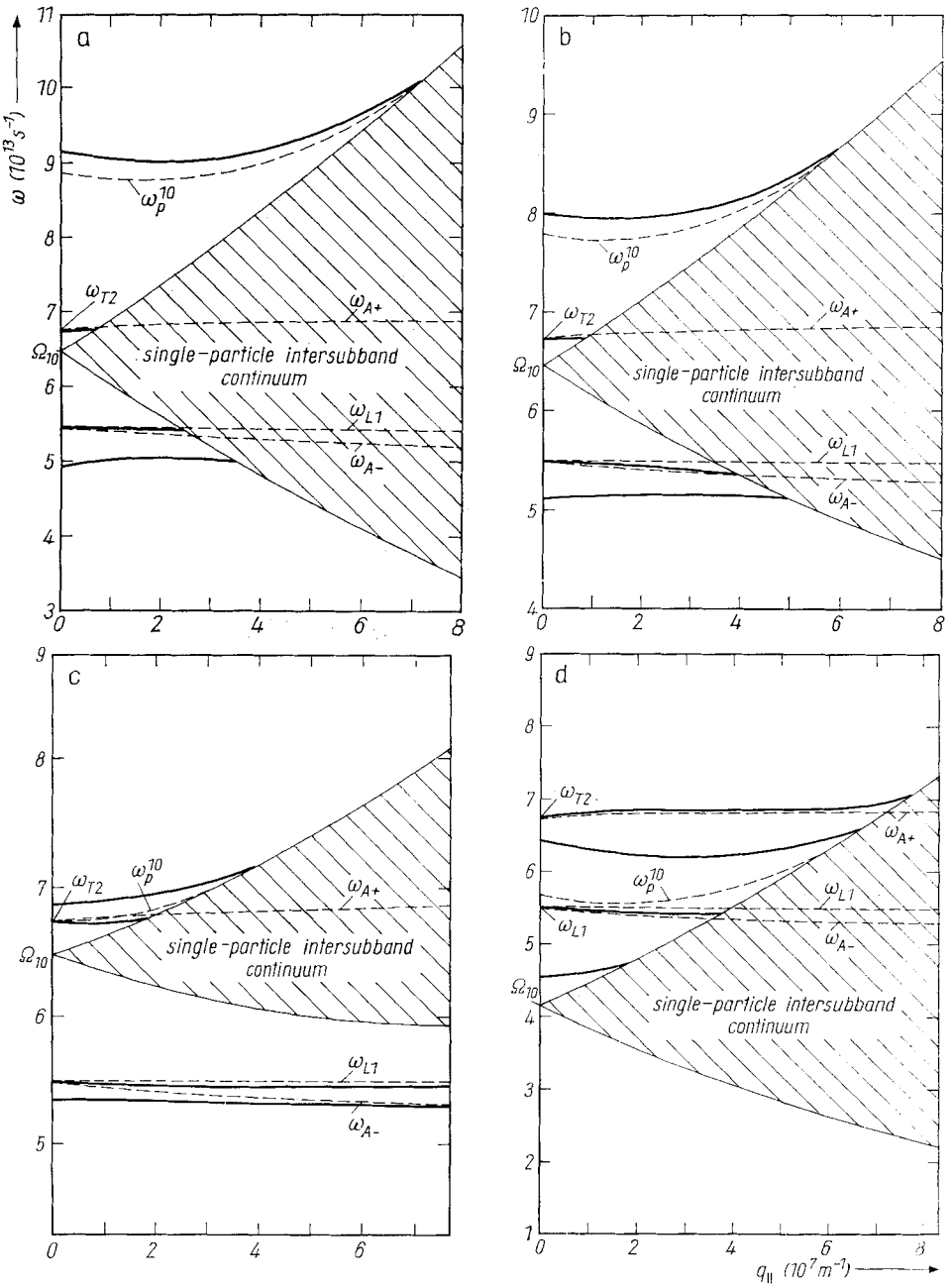

Fig. 12. Dispersion relation of the coupled (1–0) intersubband plasmon–phonons in RPA of the GaAs–$Ga_{0.75}Al_{0.25}As$ DHS (solid lines) for a) $n_{2DEG} = 1 \times 10^{12}$ cm^{-2}, $a = 20$ nm; b) $n_{2DEG} = 5 \times 10^{11}$ cm^{-2}, $a = 20$ nm; c) $n_{2DEG} = 1 \times 10^{11}$ cm^{-2}, $a = 20$ nm; d) $n_{2DEG} \times 5 \times 10^{11}$ cm^{-2}, $a = 25$ nm. The dispersion relation of the uncoupled modes is given by the dashed lines

(1–0) intersubband plasmons ω_p^{10} couple only to the LO phonons of the GaAs layer and to the antisymmetric interface phonons, but not to the symmetric one. The uncoupled phonon modes ω_{L1} and ω_{A-} are degenerated at $q_{||} = 0$. This degeneracy is lifted by the coupling of the intersubband plasmon mode ω_p^{10} with the phonon modes. For low sheet carrier concentrations it is possible that some of the coupled intersubband plasmon–phonon modes do not penetrate the single-particle intersubband continuum. Consequently, these modes are undamped in the whole range of $q_{||}$ (cf. Fig. 12 c). This is true since the intersubband modes are undamped within the single-particle intrasubband continuum due to the approximation used. The subband separation $\hbar\Omega_{10}$ varies as a function of the thickness a of the GaAs layer, whereas the frequency region, in which the phonon-like modes exist, is relatively fixed by the reststrahlen branches of the two media of the DHS. For high values of a all the four coupled (1–0) intersubband plasmon–phonons modes lie above Ω_{10} and penetrate the single-particle intersubband continuum. The influence of the sheet carrier concentration and the layer thickness on the coupled intersubband modes is significant resulting in the interesting fact that the damping of these modes strongly depends on the concentration of the Q2DEG and on the thickness of the GaAs layer. The dependence of the dispersion curves of the intersubband modes is more pronounced than in the case of the intrasubband modes.

In Fig. 13 we have plotted the dispersion curves of the coupled (1–0) intersubband plasmon–phonon modes using the LWA result for $\chi_1^{(1)}(\boldsymbol{q}_{||}, \omega)$ [11]. It is seen that the LWA result appreciably differs from that obtained in RPA. The dispersion relation (57) contains some special cases. If we expand $\chi_1^{(1)}(\boldsymbol{q}_{||}, \omega)$ in (48) to $O(q_{||}^2)$ and use for (42)

$$V_{11}^{\infty}(\boldsymbol{q}_{||}) = \frac{\hbar\Omega_{10}}{2n_{2DEG}} [\alpha_{11} - \mu_{11} q_{||} - \gamma_{11} q_{||}^2] + O(q_{||}^3) \tag{61}$$

with

$$\alpha_{11} = -\frac{n_{2DEG}}{\hbar\Omega_{10}} \frac{e^2}{\varepsilon_0 \varepsilon_{\infty 1}} \int \mathrm{d}z \int \mathrm{d}z' \, \varphi_1^*(z) \, \varphi_0(z) \, |z - z'| \, \varphi_1^*(z') \, \varphi_0(z') \,, \tag{62}$$

$$\mu_{11} = \frac{n_{2DEG}}{\hbar\Omega_{10}} \frac{e^2}{\varepsilon_0 \varepsilon_{\infty 1}} z_{10}^2; \qquad z_{10} = \int \mathrm{d}z \, \varphi_1^*(z) \, z \varphi_0(z) \,, \tag{63}$$

$$\gamma_{11} = \frac{n_{2DEG}}{\hbar\Omega_{10}} \frac{e^2}{6\varepsilon_0 \varepsilon_{\infty 1}} \int \mathrm{d}z \int \mathrm{d}z' \, \varphi_1^*(z) \, \varphi_0(z) \, |z - z'|^3 \, \varphi_1^*(z') \, \varphi_0(z') \,, \tag{64}$$

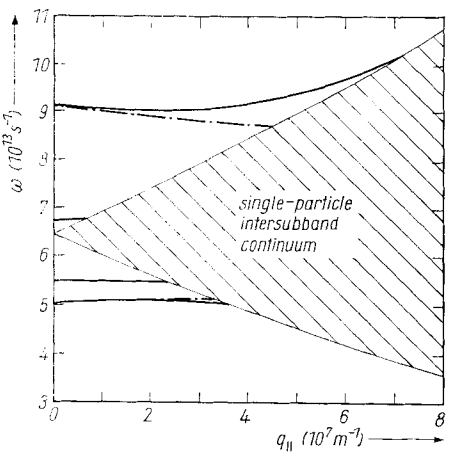

Fig. 13. Dispersion relation of the coupled (1–0) intersubband plasmon–phonons in RPA (solid lines) and in LWA (dash-dotted lines) of the GaAs–$Ga_{0.75}Al_{0.25}As$ DHS for $n_{2DEG} = 1 \times 10^{12}$ cm^{-2} and $a = 20$ nm

if we neglect the phonon contribution, the explicit dispersion relation of the intersubband plasmons follows:

$$\omega_p^{10} = \left\{(1+\alpha_{11})\,\Omega_{10}^2 - \mu_{11}\Omega_{10}^2 q_{||} + \left[\frac{\hbar\Omega_{10}}{m}\left(1+\frac{1}{2}\,\alpha_{11}\right) + v_F^2\left(\frac{1}{\alpha_{11}}+\frac{3}{4}\right) - \Omega_{10}^2\gamma_{11}\right] q_{||}^2\right\}^{1/2} \tag{65}$$

which was obtained in [3]. In the zero-order term, the extra term $\alpha_{11}\Omega_{10}^2$ is due to the depolarization effect, which results from the resonance screening in the quantum well. The linear term in $q_{||}$ is just the electrostatic energy due to the density fluctuations in the well. For the DHS one obtains

$$\alpha_{11} = \frac{n_{2DEG}}{\hbar\Omega_{10}}\,\frac{e^2}{\varepsilon_0\varepsilon_{\infty 1}}\,\frac{10a}{9\pi^2}\,, \tag{66}$$

$$\mu_{11} = \frac{n_{2DEG}}{\hbar\Omega_{10}}\,\frac{e^2}{\varepsilon_0\varepsilon_{\infty 1}}\,\frac{256a^2}{81\pi^4}\,, \tag{67}$$

$$\gamma_{11} = -\frac{n_{2DEG}}{\hbar\Omega_{10}}\,\frac{e^2}{\varepsilon_0\varepsilon_{\infty 1}}\,\frac{46a^3}{81\pi^4}\,. \tag{68}$$

The depolarization shift is seen in the Fig. 12 to 14. In Fig. 14 we have plotted the dispersion curves of the uncoupled (1–0) intersubband plasmons using the RPA and the LWA for $\chi_1^{(1)}(\boldsymbol{q}_{||}, \omega)$ in (57) and using (65) with (66 to 68).

Within the LWA it is possible to calculate the dispersion relation of the coupled excitations for the special case of intersubband plasmon–3D LO phonon coupling in an explicite form. If we expand $\chi_1^{(1)}(\boldsymbol{q}_{||}, \omega)$ and take the first non-vanishing terms we find from (55) and (57)

$$\omega_\pm = \{\tfrac{1}{2}\left((\omega_{L1}^2 + \Omega_{10}^2(1+\alpha_{11}-\mu_{11}q_{||})\right) \pm [(\omega_{L1}^2 + \Omega_{10}^2(1+\alpha_{11}-\mu_{11}q_{||}))^2 - \\ - 4\Omega_{10}^2(\omega_{L1}^2 + \omega_{T1}^2(\alpha_{11}-\mu_{11}q_{||}))]^{1/2}\}^{1/2}\,. \tag{69}$$

Analogeous to the dispersion relation (60) this restrictive approximation (69) is the mostly used one when dynamical phonon effects on the intersubband plasmons are treated [3].

6. Concluding Remarks

In this paper we have presented a detailed survey of the collective excitations in DHS's. Using the theory of dynamical screening and electron–phonon interaction in layered media [11] we discuss the uncoupled modes: long-wave optical phonons (both interface and LO phonons), intra- and intersubband plasmons, and their coupling. In distinction to most works done in this field up to now, we include the

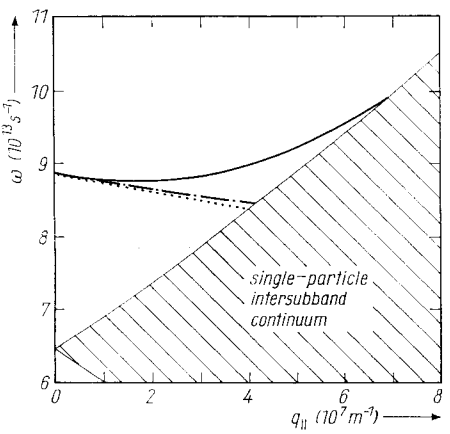

Fig. 14. Dispersion relation of the (1–0) intersubband plasmon in RPA (solid line), LWA (dash-dotted line), and calculated from the explicit dispersion relation (65) (dotted line) of the GaAs–$Ga_{0.75}Al_{0.25}As$ DHS for $n_{2DEG} = 1 \times 10^{12}$ cm^{-2} and $a = 20$ nm

effects of the interfaces on the collective excitations. We have considered the dispersion curves in different approximations, RPA, PPA, and LWA and showed that for high sheet carrier concentrations and small thicknesses of the well width of the GaAs layer the RPA results appreciably differ from those in PPA and LWA. The important fact is shown that the Landau damping of the intersubband excitations depends strongly on the thickness of the GaAs layer. Our results reduce to results of other authors calculated previously in the appropriate limits. Some of the questions, which are not answered in this paper, are:

(i) is the RPA result good enough to describe correctly the dispersion curves, and
(ii) how strong is the influence of the coupling between intra- and intersubband and between the different intersubband excitations.

Whereas (ii) demands the consideration of a two- or three-subband model which can be done without any problems, (i) seems to be an outstanding problem for a Q2DEG. Using the self-consistent STLS approximation of Singwi et al. [27], Jonson [28] found that the RPA is a less satisfactory approximation for a strict 2DEG. But the inclusion of the realistic DHS layer structure, as done in this paper within the RPA, is very crucial within the self-consistent STLS approximation.

Acknowledgements

The authors wish to express their sincere thank to Dr. Elke Wendler for reading the manuscript and to Dr. V. G. Grigoryan for checking some of the calculations.

References

[1] A. L. FETTER, Ann. Phys. (USA) **81**, 367 (1973); **88**, 1 (1974).
[2] D. DAHL and L. J. SHAM, Phys. Rev. B **16**, 651 (1977).
[3] A. C. TSELIS and J. J. QUINN, Phys. Rev. B **29**, 3318 (1984).
[4] WU XIAOGUANG, F. M. PEETERS, and J. T. DEVREESE, Phys. Rev. B **32**, 6982 (1985).
[5] J. K. JAIN and P. B. ALLEN, Phys. Rev. B **32**, 997 (1985).
[6] W. L. BLOSS and E. M. BRODY, Solid State Commun. **43**, 523 (1982).
[7] R. H. RITCHIE, Surface Sci. **34**, 1 (1973)
[8] D. N. NEWNS, Phys. Rev. B **1**, 3304 (1970).
[9] P. J. FEIBELMAN, Progr. Surface Sci. **12**, 287 (1982).
[10] B. B. DASGUPTA and D. E. BECK, in: Electromagnetic Surface Modes, Ed. A. D. BOARDMAN, John Wiley & Sons, 1982 (p. 77).
[11] L. WENDLER and R. PECHSTEDT, phys. stat. sol. (b) **138**, 197 (1986).
[12] L. WENDLER and R. PECHSTEDT, Phys. Rev. B, in the press.
[13] F. BECHSTEDT and R. ENDERLEIN, phys. stat, sol. (b) **131**, 53 (1985).
[14] T. ANDO, A. B. FOWLER, and F. STERN, Rev. mod. Phys. **54**, 437 (1982).
[15] L. WENDLER, phys. stat. sol. (b) **129**, 513 (1985).
[16] R. FUCHS and K. L. KLIEWER, Phys. Rev. **140**, A2076 (1965).
[17] P. KLEINERT, phys. stat. sol. (b) **122**, 81 (1984).
[18] LANDOLT-BÖRNSTEIN, Zahlenwerte und Funktionen aus Naturwissenschaft und Technik, N. S., Ed. K.-H. HELLWEGE, Vol. 17a, Physik der Elemente der IV. Gruppe und der III-V Verbindungen, Ed. O. MADELUNG, Springer-Verlag, Berlin/Heidelberg/New York 1982.
[19] S. ADACHI, J. appl. Phys. **58**, R1 (1985).
[20] H. FRÖHLICH, Adv. Phys. **3**, 325 (1954).
[21] D. BOHM and D. PINES, Phys. Rev. **82**, 625 (1951).
[22] J. LINDHARD, Kgl. Danske Vid. Selsk., mat.-fys., Medd. **28**, No. 8 (1954).
[23] R. LASSNIG, Phys. Rev. B **30**, 7232 (1984).
[24] L. F. LEMMENS and J. T. DEVREESE, Solid State Commun. **14**, 1339 (1974).
[25] F. STERN, Phys. Rev. Letters **18**, 546 (1967).
[26] E. BURSTEIN, A. PINCZUK, and D. L. MILLS, Surface Sci. **98**, 451 (1980).
[27] K. S. SINGWI, M. P. TOSI, R. H. LAND, and A. SJÖLANDER, Phys. Rev. **176**, 589 (1968).
[28] M. JONSON, J. Phys. C **9**, 3055 (1976).

(Received December 22, 1986)